Robotica (2005) volume 23, pp. 101–107. © 2005 Cambridge University Press
DOI: 10.1017/S0263574704000426 Printed in the United Kingdom

A simplified propulsive model of bio-mimetic robot fish and its realization

Junzhi Yu, Shuo Wang and Min Tan

Institute of Automation, Chinese Academy of Sciences, Beijing (China) 100080
(E-mail: jzyu@compsys.ia.ac.cn)

(Received in Final Form: February 25, 2004)

SUMMARY
This paper presents a simplified kinematics propulsive model for carangiform propulsion. The carangiform motion is modeled as a serial N-joint oscillating mechanism that is composed of two basic components: the streamlined fish body represented by a planar spline curve and its lunate caudal tail by an oscillating foil. The speed of fish's straight swimming is adjusted by modulating the joint's oscillatory frequency, and its orientation is tuned by different joint's deflections. The experimental results showed that the proposed simplified propulsive model could be a viable candidate for application in aquatic swimming vehicles.

KEYWORDS: Propulsive model; Robot fish; Carangiform propulsion; Body wave

1. INTRODUCTION

It is well known that a fish in nature propels itself by the coordinate motion of its body, fins and tail, achieving tremendous propulsive efficiency and excellent maneuverability which gain the advantage over conventional marine vehicles powered by rotary propellers with the same power consumption. Nature selection has ensured that the mechanical systems evolved in fish are very efficient and fitted for their living environments. The fish, in a sense of engineering, is a distinguished AUV (Autonomous Underwater Vehicle) prototype. An overview of fish swimming and the analytical methods that have been applied to some of their propulsive mechanisms was given by Sfakiotakis *et al.*[1] and Tong.[2] In recent years, researches in propulsion and maneuvering mechanisms used by fish have demonstrated a variety of prospective utilities in undersea vehicles.[3–5] In 1994, MIT successfully developed an 8-link, fish-like machine—RoboTuna, which may be the first free-swimming robot fish in the world. RoboTuna and subsequent RoboPike projects attempted to create AUVs with increased energy savings and longer mission duration by utilizing a flexible posterior body and a flapping foil (tail fin) that exploits external fluid forces to produce thrust. In the mean time, another motivation was to answer Gray's paradox,[6] which is that a fish does not seem to have enough power to propel itself at the speed it does. Since then, based on recent progress in robotics, hydrodynamics of fish-like swimming, new materials, actuators and control technology, more and more research have focused on the development of novel fish-like vehicles.

For the convenience of description we define a robot fish as a fish-like aquatic vehicle that is based on the swimming skills and anatomic structure of a fish: primarily the undulatory/oscillatory body motions, the highly controllable fins and the large aspect ratio lunate tail. As a combination of biomechanism and engineering technology, the robot fish is a multidisciplinary field that mainly involves hydrodynamics-based control and actuation technology.

In this paper, the objective is to establish a simple propulsive model for carangiform propulsion, which guides the development of a radio-controlled, 4-link and free-swimming biomimetic robot fish. Because the fish's swimming involves hydrodynamics of the fluid environment and kinematics of the fish body, it is hard to construct a precise mathematical model by purely analytical approaches. Considering that the thrust of the fish is adjusted by the joints' oscillatory frequency and its orientation of advance by the body's bend, an N-joint oscillating mechanism is employed to describe the motion of fish in our model. The speed of fish's straight swimming is adjusted by modulating for joint's oscillatory frequency, and its orientation is tuned by different joint's deflection. Based upon this model, a free-swimming biomimetic robot fish is built to experimentally verify our ideas.

The paper is organized as follows: A brief review of previous related work on carangiform propulsion is introduced in Section 2. A simplified propulsive model for carangiform propulsion is described in Section 3. Then a free-swimming biomimetic robot fish is developed to validate the former model. Finally, conclusions and ideas about future work are drawn.

2. PREVIOUS RELATED WORK

BCF (body and/or caudal fin) swimming movements are usually categorized into anguilliform, subcarangiform, carangiform and thunniform mode, basically according to the wavelength and the amplitude envelope of the propulsive wave underlying the fish's behavior.[1] In a broader context, recent studies on the robot fish primarily concentrate on the anguilliform swimming mode and the caragiform swimming mode. During the anguilliform locomotion, the whole body participates in large amplitude undulations, which is common in eels and lampreys. For the carangiform locomotion, the body's undulations are entirely confined to the last third of the body, and thrust is produced by means of a rather stiff caudal fin. Compared to anguilliform swimmers,

https://doi.org/10.1017/S0263574704000426 Published online by Cambridge University Press

carangiform swimmers are generally faster, but with less agility due to the relative rigidity of their bodies. Also, carangiform propulsion is more convenient for engineering realization.

To some extent much more interest of investigations focuses on the carangiform locomotion. Some theoretical and experimental studies have explored the possibility of applying the carangiform propulsive mechanism for aquatic vehicles. Early resistive hydrodynamic models[7] were based on a quasi-static approach that uses steady-state flow theory to calculate the fluid forces. Later models dealt with more realistic fish-type motions, Wu[8] originally developed a 2-D waving plate theory, treating fish as an elastic plate. Thereafter elongated-body theory[9, 10] and large-amplitude elongated-body theory[11, 12] that are suited to carangiform swimming were formed. These linear or nonlinear extensions of the waving plate theory allow an analysis of fast starts, as well as steady swimming.

At present, some artificial systems are developed to investigate fish-like locomotion mechanism. In particular, oscillating foil has been proposed as an alternative propulsor to the conventional screw propeller.[3,13,14] The development of 8-link, foil-flapping robotic mechanisms (Robotuna)[3,15,16] required detailed measurements of the forces on an actively controlled body. Harper *et al.*[17] proposed the design of optimal spring constant to actuate the oscillating foil. Kelly *et al.*[18] proposed a model for planar caragngiform swimming based on reduced Euler-Lagrange equations for the interaction of a rigid body and an incompressible fluid. Mason *et al.*[19] built a three-link robot system to study carangiform-like swimming. They experimentally verified a quasi-steady fluid flow model for predicting the thrust generated by flapping tail. These interesting investigations made good progress in carangiform propulsion. However, there is much work to do in both integration of the theories and applicability of the real aquatic mechanisms. This paper involves an improved approach to design a robot fish based on a simplified kinematics model that relates frequency to speed and joint angle bias to turns, where geometric reduction is employed and complex hydrodynamic analysis is avoided. At the same time, a biomimetic robot fish prototype was designed, which is easy to made.

3. A SIMPLIFIED PROPULSIVE MODEL FOR CARANGIFORM PROPULSION

This paper concentrates on the lateral motion of fish body, which is in the form of a traveling wave smoothly increasing from the front to the tail end. The method employed is a discretized numerical fitting. It is shown in literature[1] that the passage of a wave underlies the fish's propulsive structure. The propulsive wave behaves as lateral curvature in spine and musculature, which begins behind the head and increases with amplitude as it moves to the back. It traverses at a speed greater than the forward speed. Based on this information, as shown in Fig. 1, a physical model of the carangiform motion can be divided into two parts: flexible body and oscillatory lunate caudal fin, where the flexible body is represented by a series of oscillatory hinge joints, and the caudal fin by an oscillating foil. A relative swimming model for the RoboTuna

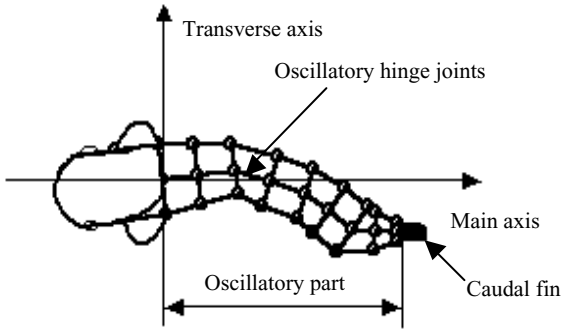


Fig. 1. Physical model of fish swimming.

(carangiform) has been presented by Barrett *et al.*,[16] whose undulatory motion is assumed to take the form of a traveling wave (Eq.1) originally suggested by Lighthill.[9]

$$y_{body}(x, t) = [(c_1 x + c_2 x^2)][\sin(kx + \omega t)] \qquad (1)$$

where y_{body} is the transverse displacement of body, x is the displacement along main axis, k is the body wave number ($k = 2\pi/\lambda$), λ is the body wave length, c_1 is the linear wave amplitude envelope, c_2 is the quadratic wave amplitude envelope, ω is the body wave frequency ($\omega = 2\pi f = 2\pi/T$).

There is no standard technique for the quantitative analysis of the carangiform motion that encompasses various external forces and torques due to hydrodynamic forces, gravitational forces, buoyant forces, etc. In this section, the kinematics of the carangiform motion will only be discussed depending on the specified propulsive wave, i.e. the above body-wave equation. Given the equation, the next task is to determine the proper body-wave parameters (i.e. c_1, c_2, k, ω, etc.) for a desired swimming motion in terms of some criteria. In the literature,[16] a set of seven key parameters for the kinematics model of a RoboTuna was found and a genetic algorithm was used to guide the search for an optimal swimming efficiency. But for various species, dimensions, and shapes of fish, there are different parameter sets to adapt themselves to the surroundings. Consequently, it is an exceedingly tough task to optimize the fish's swimming efficiency and/or maneuverability.

For simplicity, a discrete planar spline curve parameterized as "sinusoid" is taken into account, i.e. the time variable t is separated from the body-wave function $y_{body}(x, t)$. That is to say, the traveling body-wave is decomposed into two parts: (a) the time-independent spline curve sequences $y_{body}(x, i)$ ($i = 0, 1, \ldots, M-1$) in an oscillation period, which is described by Eq.(2), and (b) the time-dependent oscillating frequency f, which is described as the times of recurring oscillation at the unit time interval.

$$y_{body}(x, i) = [(c_1 x + c_2 x^2)]\left[\sin\left(kx \pm \tfrac{2\pi}{M} i\right)\right] \qquad (2)$$

where i denotes the ith variable of the spline curve sequence $y_{body}(x, i)$, M is called body-wave resolution that represents the discrete degree of the overall traveling wave, which is restricted by the maximum oscillating frequency

https://doi.org/10.1017/S0263574704000426 Published online by Cambridge University Press

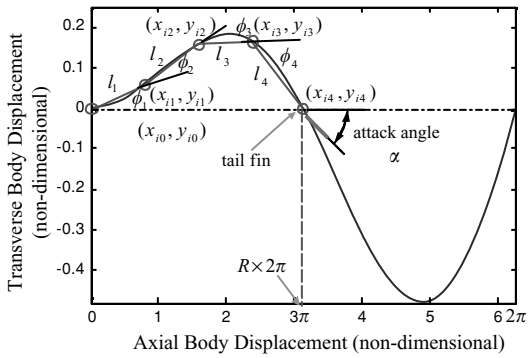


Fig. 2. Link based body-wave fitting.

of actuators. It should be noticed that the "+" sign or the "−" one has the same effect on the sequence $y_{body}(x,i)$ in an overall oscillation period, but their initial moving direction is different due to different initial values. Note that the "−" sign is used in this paper.

Considered that the oscillatory part of a fish consists of many rotating hinge joints, as shown in Fig. 2, it can be modeled as a planar serial chain of links along the axial body displacement. The position of each link in the moving chain can then be achieved by numerical fitting. Before fitting the body-wave curve, we define the relative wavelength R as the length ratio of wavelength exhibited by the fish's oscillatory part to that of a whole sine wave. If assuming the full fish-body exhibits a whole propulsive wave at $k=1$, R will be identical with the length ratio of the fish's oscillatory part to that of the fish-body, which typically characterizes the fish as anguilliform, subcarangiform, carangiform and thunniform. When R approaches zero, to some extent, the fish's oscillatory part may be viewed as a rigid rod that hardly produces any thrust; when R nears to 0.5, half a sine wave is present in the oscillatory part during locomotion. With the purpose of mimicking carangiform motion, R is empirically around 1/3. To expand the maneuverability and facilitate the realization of the fish-like mechanical system, actually a larger value, e.g. 0.5, can be chosen.

As mentioned above, since the wavelength of a whole propulsive wave is viewed as 2π at $k=1$, the wavelength of the oscillatory part at R is then $R\times 2\pi$. On the assumption that the fish-like mechanical system is to be made up of N joints and the body-wave resolution is M, the body wave at an interval of 0 to $R\times 2\pi$ along the axial body displacement can be fitted with a N-link mechanism. Let the length of each link be l_j $(j=1,2,\ldots,N)$, to keep it non-dimensional, the ratio of the links must be normalized to be independent of its actual size, i.e. $l_1 : l_2 : \ldots : l_N = m[l'_1 : l'_2 : \ldots : l'_N]$, where m denotes the length factor, l'_j indicates the normalized length of the jth link, and especially l'_1 equals 1.0. Also let two end-point coordinate pairs of each link l'_j be (x_{j-1}, y_{j-1}) and (x_j, y_j), respectively, and the joint angle between l'_{j-1} and l'_j be ϕ_j. Then once the amplitude coefficients (i.e. c_1 and c_2) and k are determined, the shape of the propulsive wave at some time will be found. Mathematically, the jth link's joint angle ϕ_{ij} at the time of ith $(i=0,1,\ldots,M-1)$ can be calculated by fitting the current wave. The following problem is to search an appropriate joint angle ϕ_{ij} to meet the condition that the end-point of the link l'_j falls into the wavy curve and the x-coordinate of the last link's endpoint (x_{iN}, y_{iN}) just equals $R\times 2\pi$. That is to say, it must satisfy the constraint condition given by:

$$\begin{cases} (x_{i,j}-x_{i,j-1})^2+(y_{i,j}-y_{i,j-1})^2 = l'^2_j \\ y_{i,j} = \left(c_1 x_{ij} + c_2 x_{ij}^2\right)\sin\left(k x_{ij} - \frac{2\pi}{M} i\right) \end{cases} \tag{3}$$

where the subscript i indicates the ith time of the oscillating sequence, and j denotes the jth link. Through a series of numerical iterative operations, the end-point coordinate pair $(x_{i,j}, y_{i,j})$ can be calculated. Then the slope of each link l'_j at the arbitrary ith time can be computed. Finally, as illustrated in Eq. (4), a two-dimensional rectangular array OscData$[M][N]$ for the joint angle ϕ_{ij} is obtained, which will be used as the primitive oscillating data of the robot fish. Based on this oscillatory array, the fish body's shape can geometrically be changed by adding different deflections $\Delta\phi_i$ to the first N' $(0<N'<N)$ joints, the corresponding oscillatory array OscData$'[M][N]$ is shown in Eq. (5). The motion orientation of the fish varies with the unstable shape in a limited cycle due to a complex hydrodynamic interaction, so called added mass effect.

$$\text{OscData}[M][N] = \begin{pmatrix} \phi_{01} & \phi_{02} & \cdots & \phi_{0N} \\ \phi_{11} & \phi_{12} & \cdots & \phi_{1N} \\ \cdots & \cdots & \cdots & \cdots \\ \phi_{M-1,1} & \phi_{M-1,2} & \cdots & \phi_{M-1,N} \end{pmatrix} \tag{4}$$

$$\text{OscData}'[M][N] = \begin{pmatrix} \phi_{01}+\Delta\phi_1 & \phi_{02}+\Delta\phi_2 & \cdots & \phi_{0,N'-1}+\Delta\phi_{N'-1} & \phi_{0N'} & \cdots & \phi_{0N} \\ \phi_{11}+\Delta\phi_1 & \phi_{12}+\Delta\phi_2 & \cdots & \phi_{1,N'-1}+\Delta\phi_{N'-1} & \phi_{1N'} & \cdots & \phi_{1N} \\ \cdots & \cdots & \cdots & \cdots & \cdots & \cdots & \cdots \\ \phi_{M-1,1}+\Delta\phi_1 & \phi_{M-1,2}+\Delta\phi_2 & \cdots & \phi_{M-1,N'-1}+\Delta\phi_{N'-1} & \phi_{M-1,N'} & \cdots & \phi_{M-1,N} \end{pmatrix} \tag{5}$$

We next assume that the full control of a fish relies on the internal shape (the joint angle ϕ_{ij}) for maneuverability and the oscillating frequency f of the tail for speed. There are some reasons for this choice, although a fish in nature is observed to use a combination of amplitude and frequency for speed control. Firstly, the fish's motion, in essence, is governed by its velocity whose magnitude is the body's speed and whose direction is the body's direction of motion. The separation of speed and direction will contribute itself to the actual motion control with different methods. Secondly, only the relating frequency to speed is easily realized in the control. We also attempt to increase the amplitude during changing frequency, but an acute increase in amplitude often leads to malfunction of running servomotors with high frequency, which is probably due to poor quantitative understanding of the role of the amplitude plays in the speed control, as well as the limited rotation range of the servomotor. Finally, as will be shown in the following section, a robot fish controlled in this method can adequately reproduce a carangiform-like motion and obtain a certain level of maneuverability. Based on the success and failure of this design,

https://doi.org/10.1017/S0263574704000426 Published online by Cambridge University Press

it can be concluded that a robot fish actuated by servomotors is feasible but not ideal, and that a more flexible actuator will perhaps be needed to mimic the full motion of fish in nature.

Since the mechanical robot fish is equipped with four links, all calculations and experiments in this paper are carried out on a 4-link model. The schematic of the link-based body-wave fitting has been shown in Fig. 2. Because the tail fin is attached to the last link, the angle α derived from the slope of the last link is just the fin's attack angle. The body-wave parameters we have chosen are as follows: $c_1 = 0.1$, $c_2 = 0.05$, $k = 1$, $R = 0.5$, $l'_1 : l'_2 : l'_3 : l'_4 = 1 : 1 : 0.8 : 0.6$, $M = 18$, and $N = 4$. Regarding the selection of amplitude coefficients c_1 and c_2, it must be noted that the maximum sideways tail motion for the elongate mode is approximately 20% of the fish length,[20] i.e. satisfying the constraint give by:

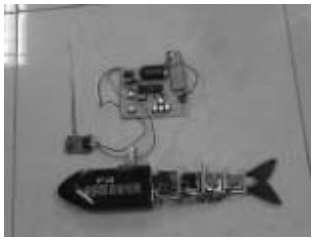
$$\max(2|c_1 x + c_2 x^2|) < 0.2BL \tag{6}$$

where BL denotes the body length of the robot fish. In general, the more the number of the links, the better the mechanism's maneuverability and redundancy, but the harder the control and construction of the robot. In a synthetic way, 2-6 links are perhaps appropriate for the robot fish design. The increasing length of the links improves its flexibility and suppleness; however, the robot fish would have reduced motion agility. In a strict way, such a robot fish design based on the above parameters may not be carangiform, since both theoretical and practical factors have to be synthesized during realization.

As mentioned before, the eventual results for the propulsive wave fitting, according to the given parameters, are a 2-D 18×4 rectangular array of joint angles and the oscillating frequency, which are independent of the fish's dimensions and shapes. Therefore, a parameters set $\{\phi_{i1}, \phi_{i2}, \phi_{i3}, \phi_{i4}, f\}$ is chosen to control the fish's motion. The speed of the fish's straight motion is adjusted by modulating the joint's oscillating frequencies, and its orientation is tuned by different joint's deflection (for detailed control method, see section 4).

4. BIOMIMETIC ROBOT FISH BASED ON THE SIMPLIFIED PROPULSIVE MODEL

On the basis that fundamental physics are preserved between biological model and artificial system, we decided to construct an experimental biomimetic robot fish system based on the simplified propulsive model for carangiform swimming. In 2001, a radio-controlled, 4-link biomimetic robot fish was developed by the Laboratory for Complex Systems and Intelligence Science of Chinese Academy of Sciences and the Robotic Institute in Beijing University of Aeronautics and Astronautics, which is 400 mm in length, 40 mm in width and 78 mm in thickness. The main objective of developing such a robot fish was to build an experimental system that has the following functions: (a) to verify the proposed simplified propulsive model for carangiform swimming, (b) to demonstrate the feasibility of utilizing the tail fin for both propulsion and turning, and (c) to allow for experimental determination of operating parameters that make fish more maneuverable at various speeds.



(a) Robot fish prototype and its remote controller



(b) Swimming robot fish vs. real fish (Carp)

Fig. 3. Top view of a robot fish.

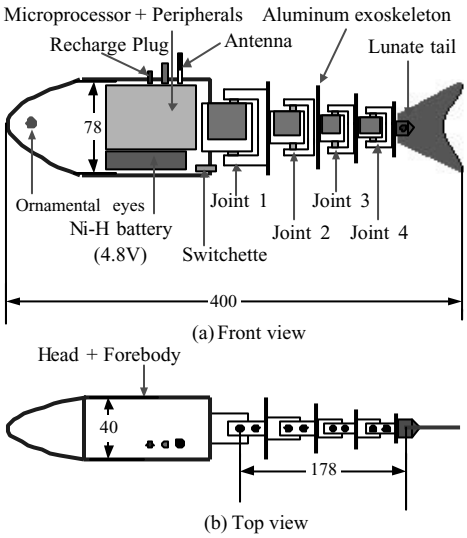


Fig. 4. Mechanical configuration of the robot fish.

4.1. Basic configuration

The robot fish prototype that we are currently developing is presented in Fig. 3. It is controlled by a remote controller shown in Fig. 3 (a). Fig. 3 (b) shows that it swims like a real carp fish in a tank. As shown in Fig. 4, the robot fish primarily consists of:

- Control unit (microprocessor + peripherals)
- Communication unit (wireless receiver)
- Support (aluminum exoskeleton + head + forebody)
- Actuation unit (DC servomotors)
- Accessories (battery, waterproofed skin, tail fin)

Based on a hydrodynamic analysis, a hollow, streamlined, rigid head and forebody are molded using fiberglass, which allows for larger space to house electrical and communication components. In order to swim in a small experimental water pond, the built fish has to be as compact as possible. The onboard microprocessor, additional peripherals, wireless

https://doi.org/10.1017/S0263574704000426 Published online by Cambridge University Press

Table I. Technical parameters of the robot fish prototype.

Size (L × W × H)	∼400 × 40 × 78 mm^3
Weight	∼0.5 kg
Number of joints	4
Max oscillating frequency	2 Hz (in water)
Length of oscillatory part	178 mm
Maximum speed	∼0.32 m/s
Minimum turning radius	∼200 mm
Maximum torque	3.2 kgf × cm
Working voltage	4.8 v
Drive mode	DC servomotor
Control mode	Radio control (315 M)

receiver and power supply are hence put in the cell of the fish's forebody.

Four DC servomotors acting as the actuator of joints are linked to the aluminum exoskeleton. A lunate foil is attached to the fourth link, which serves as the tail fin. The installation position of the joints and the size of the tail are referred to the shape of a grass carp. In the meantime, some steel balance weights are located in the forebody and lower side of the exoskeleton to adjust the balance of gravitational to the and buoyant forces.

To guarantee the fish to be waterproofed, its overall posterior part is covered up by a rippled rubber tube, i.e. waterproofed skin, which is sealed upon the fiberglass forebody. A recharge plug is on the top section of the fish for recharging the batteries. Because the underwater wireless communication is very difficult to realize, after some communication malfunction, the idea of submerging fish to a constant depth is not realistic. In the following tests or experiments, the robot fish is partly submerged, namely, the tail fin is submerged in the water and the antenna is extended to the surface. Under this circumstance, the un-modelled effects such as uneven gravitational effects, surface waves and finiteness of the water tank should be taken into account in the design of our control system. It is noted that in a real aquatic vehicle, such unfavorable factors will be mitigated, or even not exist.

4.2. Control system and control performance

In the fish's control unit, the servomotors are controlled by an onboard microprocessor and a CPLD (complex programmable logic device). The speed of fish's straight motion is adjusted by modulating the joint's oscillating frequency, and its orientation is tuned by different joint's deflection. Adding various deflections, plus or minus, to the joint angles ϕ_{i1} and ϕ_{i2} in each oscillation period, different motional direction is achieved. The basic technical parameters of the robot fish prototype are described in Table I.

Through a wireless receiver, the commands from the upper level are transformed to an oscillating frequency and rotation angles of the servomotors that are adjusted by PWM (pulse width modulation) signals generated from CPLD. Recently, two control modes have been developed for the prototype: the manual mode and the automatic control mode.

- For the manual mode, a remote controller imitating a game joystick is developed, as shown in Fig. 3 (a). The fish is able to accelerate, decelerate, turn right and turn left by pressing keys: UP/DOWN (for speed control) and LEFT/RIGHT (for orientation control).
- In the automatic control mode, an overhead vision system is adopted to control the robot fish in a closed loop. A CCD camera hung over the swimming pond acts as a sensor captures the fish's motion and surrounding information, which provide a real-time visual feedback. The speed of straight swimming and turning performance, by means of on-line visual feedback of the fishes' position and orientation, are then evaluated.

Table II. Oscillating frequency (Hz) vs. speed (m/s) of straight swimming.

Frequency	0.5	0.57	0.67	0.8	1.0	1.34	2.0
Speed	0.12	0.16	0.18	0.20	0.23	0.26	0.32

Table III. Angular speed (radian/s) at $f = 2$ Hz.

Deflections	−30	−22.5	−15	−7.5	0	7.5	15	22.5	30
Angular speed	−1.2	−0.92	−0.8	−0.5	−0.1 ∼ 0.1	.4	.75	.95	1.1

Based upon the experimental data, the relationship between the oscillating frequency f and the straight swimming speed V is shown in Table II and Fig. 5. It is observed that the maximum swimming speed is near to 0.32 m/s, i.e. about 0.8 times of body length per second, at the frequency of 2 Hz with a lunate tail fin. In contrast to a real fish, such a swimming efficiency is not high due to large friction resistance between the oscillatory part and water. However, there is a general tendency for the swimming speed to increase with the oscillating frequency. For a practical reason, the speed cannot be infinitely expanded since the servomotors can hardly follow sufficiently high speeds in high oscillating frequency areas.

Further more, as an essential element of maneuverability, the turning performance of the fish is measured. Table III shows the experimental results for an angular speed at $f = 2$ Hz. The fish is required to round a 2π circle with different turning radii in the experiments, and corresponding angular speeds are obtained. During the measurements, 8 directional levels are sampled at intervals of 7.5°. The corresponding deflection in degrees is added to the first two joint angles (ϕ_{i1}, ϕ_{i2}) in each oscillation period; accordingly, the fish body deflects to one side. It is also attempted to

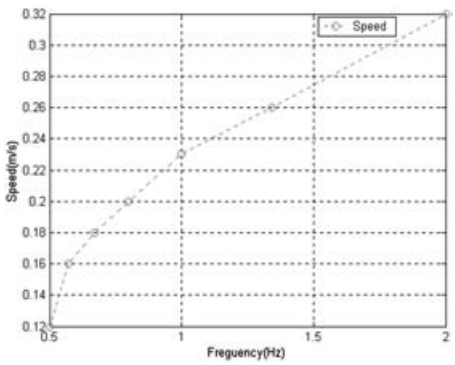
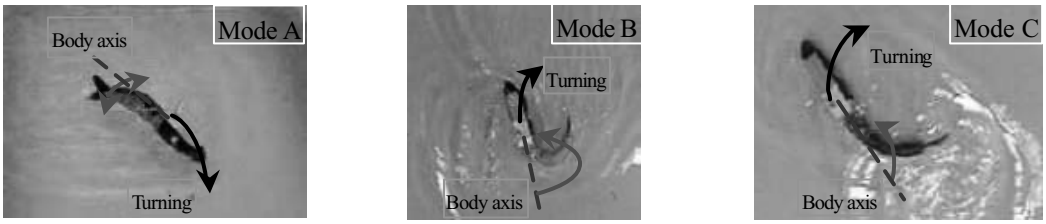


Fig. 5. Oscillating frequency vs. swimming speed.

https://doi.org/10.1017/S0263574704000426 Published online by Cambridge University Press



(a) Turning during advancing (b) Snap turning (c) Turning from rest

Fig. 6. Three basic turning modes of robot fish.

add deflections to the last two joints (ϕ_{i3}, ϕ_{i4}), but some differences of the turning radius are found. In this paper, only deflections added to the first two joints are discussed. As seen from Table III, the angular speed increases with the increase of deflections, and the values of the angular speed are not quite symmetric with a bias. This problem seems to indicate that the current system lacks mechanical symmetry due to joint binding, motor installation, and so on.

Three basic turning modes for a fish propelled only with oscillating tail fin were initially discussed by Hirata *et al*.,[21] and are then redefined as follows.

■ **Mode A**: turning during advancing (see Fig. 6 (a)). In this mode, the robot fish intentionally deflects its body only to one side by exerting a geometric bias during advance, where a head and forebody of the fish are equivalent to a rudder and its last two links and the tail fin function as a screw propeller of the ship. This is a fundamental turning mode in that the robot fish can turn at various turning-radii and speeds in this manner.

■ **Mode B**: snap turning (see Fig. 6 (b)). The robot fish, using this mode, suddenly bends its body to a "C" sharp and keeps the posture during motion, i.e. all the joints synchronously reach their left/right oscillatory limits. As it is well known, C-shaped and S-shaped movements are important for most fishes when escaping predators and for some fish to achieve prey capture.[22] The remaining kinetic energy and hydrodynamic forces jointly act on the C-shaped fish body so that its motion direction changes drastically, and its turning radius is the smallest of three modes. Therefore, this turning mode is very effective in occasions needed high maneuverability or fast-turn. For our robot fish prototype, its snap turning radius is about 0.5BL and the angular speed around 1.0 radian/s.

■ **Mode C**: turning from rest (see Fig. 6 (c)). The robot fish, in this case, deflects its body only to one side swiftly from a stationary state. The inertia force and friction force of the fish body and the tail fin are changed to the moment of rotation, and the fish turns quickly. This mode is also suitable for fast start and directional adjustment with large-angle, but its turning speed and turning angle are difficult to control accurately in practice.

After performing some simple movements such as going forward, turning left and turning right, a high quality control system can be developed by a combination of these basic moving patterns. Considering that a parameters set $\{\phi_{i1}, \phi_{i2}, \phi_{i3}, \phi_{i4}, f\}$ can be reduced to control fish's motion in the above propulsive model, the robot fish's motion control is then decomposed into the speed control and the orientation control. The aim of the speed control is to search a certain oscillating frequency f so that the fish moves fast and steadily, while the orientation control is designed to choose appropriate joints angles $\{\phi_{i1}, \phi_{i2}, \phi_{i3}, \phi_{i4}\}$ to navigate the fish to the desired position with a certain speed. Since, as mentioned before, the shape of the fish body can be geometrically changed by the joints' bias, in a sense, the fish can be viewed as a deformable body that has nonlinear motion, i.e. the body oscillates.

5. CONCLUSIONS AND FUTURE WORK

A simplified propulsive model for carangiform swimming has been presented, whose eventual results are a 2-D rectangular array of joint angles and the oscillatory frequency. Based on this model, a radio-controlled, 4-link and free-swimming biomimetic robot fish has been developed. The speed of fish's swimming is adjusted by modulating the joints' oscillatory frequency, and its orientation is tuned by different joint's deflections. Experimental measurements partially verified the feasibility of the model in the application of robot fish. However, the proposed motion control algorithms did not take fish dynamics into account, only the fish's motion kinematics was considered, which has to be improved in the future.

Future work with the developed robot fish system will involve an expanded closed-loop control, and a full planar motion planning algorithm for complex and cluttered environments with obstacles based on visual feedback. Under such circumstance proper and efficient speed control algorithm and orientation control algorithm are essential for the fish's stable motion in aquatic environments. At the same time, a 3-D propulsive model has to be investigated if a new degree of freedom (Up/Down) is planned to be added to the robot fish, which enables the robot fish to navigate in a 3-D workspace.

Acknowledgement

This work is funded by research grants from the robotics subject of 863 Program (Grant No. 2001AA422370) and important project of Basic Science (Grant No. 2001CCA02900). The authors would like to thank the referees for a careful reading of the manuscript and for their helpful comments.

References

1. M. Sfakiotakis, D. M. Lane and J. B. C. Davies, "Review of fish swimming modes for aquatic locomotion," *IEEE Journal of Oceanic Engineering* **24**, 237–252 (1999).

https://doi.org/10.1017/S0263574704000426 Published online by Cambridge University Press

2. B. G. Tong, "Propulsive mechanism of fish's undulatory motion," *Mechanics In Engineering* **22**, 69–74 (2000) (in Chinese).
3. M. S. Triantafyllou and G. S. Triantafyllou, "An efficient swimming machine," Scientific American, 64–70 (1995).
4. J. M. Anderson, M. S. Triantafyllou and P. A. Kerrebrock, "Concept design of a flexible-hull unmanned undersea vehicle," *Proceedings of the International Offshore and Polar Engineering Conference* (1997) pp. 82–88.
5. Mojarrad Mehran, "AUV biomimetic propulsion," *Oceans Conference Record (IEEE)* (2000) pp. 2141–2146.
6. J. Gray, "Studies in Animal Locomotion, VI. The Propulsive Powers of the Dolphin," *J. Exp. Biol.* **13**, 192–199 (1936).
7. G. Taylor, "Analysis of the swimming of long narrow animals," *Proc. R. Soc. Lond, Ser.* **A 214**, 158–183 (1952).
8. T. Y. Wu, "Swimming of a waving plate," *J. Fluid Mech.* **10**, 321–344 (1961).
9. M. J. Lighthill, "Note on the swimming of slender fish," *J. Fluid Mech.* **9**, 305–317 (1960).
10. M. J. Lighthill, "Aquatic animal propulsion of high hydromechanical efficiency," *J. Fluid Mech.* **44**, 265–301 (1970).
11. M. J. Lighthill, "Large-amplitude elongated-body theory of fish locomotion," *Proc. R. Soc. Lond, Ser.* **B 179**, 125–138 (1971).
12. J. Y. Cheng and R. Blickhan, "Note on the calculation of propeller efficiency using elongated body theory," *J. Exp. Biol.* **192**, 169–177 (1994).
13. K. Hirata, "Development of experimental fish robot," *Sixth International Symposium on Marine Engineering* (2000) pp. 711–714.
14. J. Czarnowski, R. Cleary and B. Kreamer, "Exploring the possibility of placing traditional marine vessels under oscillating foil propulsion," *Proceedings of the Seventh International Offshore and Polar Engineering Conference* (1997) pp. 76–81.
15. D. Barrett, M. Triantafyllou, D. K. P. Yue, M. A. Grosenbaugh and M. J. Wolfgang, "Drag reduction in fish-like locomotion," *Journal of Fluid Mechanics* **392**, 183–212 (1999).
16. D. Barrett, M. Grosenbaugh and M. Triantafyllou, "The optimal control of a flexible hull robotic undersea vehicle propelled by an oscillating foil," *Proceedings of the IEEE Symposium on Autonomous Underwater Vehicle Technology* (1996) pp. 1–9.
17. K. A. Harper, M. D. Berkemeier and S. Grace, "Modeling the dynamics of spring-driven oscillating-foil propulsion," *IEEE Journal of Oceanic Engineering* **23**, 285–296 (1998).
18. S. D. Kelly and R. M. Murray, "Modelling efficient pisciform swimming for control," *Int. J. Robust and Nonlinear Control* **10**, 217–241 (2000).
19. R. Mason and J. Burdick, Experiments in carangiform robotic fish locomotion, *ICRA* (2000) pp. 428–435.
20. J. R. Hunter and J. R. Zweifel, "Swimming speed, tail beat frequency, tail beat amplitude and size in jack mackerel, Trachurus symmetricus, and other fishes," *Fishery Bulletin* **69**, 253–266 (1971).
21. K. Hirata, T. Takimoto and K. Tamura, "Study on turning performance of a fish robot," *First International Symposium on Aqua Bio-Mechanisms* (2000) pp. 287–292.
22. P. Domenici and R. W. Blake, "The kinematics and performance of fish fast-start swimming," *The Journal of Experimental Biology* 1165–1178 (1997).

https://doi.org/10.1017/S0263574704000426 Published online by Cambridge University Press